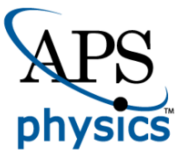

Kondo Insulator to Semimetal Transformation Tuned by Spin-Orbit Coupling

S. Dzsaber, L. Prochaska, A. Sidorenko, G. Eguchi, R. Svagera, M. Waas, A. Prokofiev, Q. Si, and S. Paschen

Phys. Rev. Lett. **118**, 246601 — Published 16 June 2017

DOI: 10.1103/PhysRevLett.118.246601

Kondo insulator to semimetal transformation tuned by spin-orbit coupling

S. Dzsaber[1], L. Prochaska[1], A. Sidorenko[1], G. Eguchi[1],
R. Svagera[1], M. Waas[1], A. Prokofiev[1], Q. Si[2], and S. Paschen[1,2,*]
[1] *Institute of Solid State Physics, Vienna University of Technology, Wiedner Hauptstr. 8-10, 1040 Vienna, Austria and*
[2] *Department of Physics and Astronomy, Rice University, Houston, Texas 77005, USA*
(Dated: May 23, 2017)

Recent theoretical studies of topologically nontrivial electronic states in Kondo insulators have pointed to the importance of spin-orbit coupling (SOC) for stabilizing these states. However, systematic experimental studies that tune the SOC parameter $\lambda_{\rm SOC}$ in Kondo insulators remain elusive. The main reason is that variations of (chemical) pressure or doping strongly influence the Kondo coupling $J_{\rm K}$ and the chemical potential μ – both essential parameters determining the ground state of the material – and thus possible $\lambda_{\rm SOC}$ tuning effects have remained unnoticed. Here we present the successful growth of the substitution series $Ce_3Bi_4(Pt_{1-x}Pd_x)_3$ ($0 \leq x \leq 1$) of the archetypal (noncentrosymmetric) Kondo insulator $Ce_3Bi_4Pt_3$. The Pt-Pd substitution is isostructural, isoelectronic, and isosize, and therefore likely to leave $J_{\rm K}$ and μ essentially unchanged. By contrast, the large mass difference between the $5d$ element Pt and the $4d$ element Pd leads to a large difference in $\lambda_{\rm SOC}$, which thus is the dominating tuning parameter in the series. Surprisingly, with increasing x (decreasing $\lambda_{\rm SOC}$), we observe a Kondo insulator to semimetal transition, demonstrating an unprecedented drastic influence of the SOC. The fully substituted end compound $Ce_3Bi_4Pd_3$ shows thermodynamic signatures of a recently predicted Weyl-Kondo semimetal.

Topological phases [1] in condensed matter systems [2, 3], most recently encompassing also gapless variants [4], continue to attract great attention. To date, work has mostly focused on weakly correlated materials, but it is clear that yet more exotic physics may be discovered in strongly correlated settings [5]. Thus, the proposal that Kondo insulators [6, 7] – some of the most strongly correlated materials – exhibit topologically nontrivial metallic surface states [8] was taken up enthusiastically and triggered many experimental studies, most notably on SmB_6 [9]. A key ingredient for a topologically nontrivial electronic structure in Kondo insulators is the strong spin-orbit coupling (SOC) of the heavy lanthanide $4f$ elements [8], but the importance of SOC of the conduction electrons that hybridize with the $4f$ electrons has also been demonstrated [10]. In studies of the periodic Anderson model, the latter was shown to tune between different phases, including topological and topologically trivial Kondo insulators [10], Dirac-Kondo semimetals [11], and most recently Weyl-Kondo semimetals [12]. To link such studies directly to experiment it would be highly desirable to find an experimental "tuning knob" for SOC in Kondo systems. The availability of parameters that tune the Kondo interaction strength has been vital to the field of heavy fermion quantum criticality [13, 14]. Here we demonstrate for the first time SOC tuning in a Kondo insulator.

In Kondo insulators the Kondo interaction between localized ($4f$ and less frequently $5f$ or $3d$) and itinerant (typically d) electrons opens a narrow gap – of the order of 10 meV – in the electronic density of states at the Fermi level [6, 7]. Among the archetypal cubic Kondo insulators that have been studied for decades [6, 7], $Ce_3Bi_4Pt_3$ appears as an ideal starting material for our study. As a Ce-based system it represents the conceptually simple situation of a single $4f$ electron as the localized species. Its Kondo insulating ground state is well established [15–17] and quite robust: The Kondo insulator gap persists up to 145 kbar [18] and is closed only for magnetic fields as high as 40 T [19]. $Ce_3Bi_4(Pt,Pd)_3$ crystallizes in a cubic structure of space group $I\bar{4}3d$ with a noncentrosymmetric unit cell containing 40 atoms [20]. All three constituting elements occupy unique crystallographic sites and form three sublattices that all lack inversion symmetry. Interestingly, mirroring Ce at the unit cell center transforms it into Pt (Pd) and vice versa (left inset in Fig. 3), reflecting the direct involvement of these elements in defining the noncentrosymmetric structure. Theoretical studies have suggested that $Ce_3Bi_4Pt_3$ hosts topologically nontrivial states [8, 27], but these could so far not be experimentally resolved [28].

Generally, chemical substitution with atoms of sizeable mass difference seems a promising route for SOC tuning because the atomic number Z (or the mass) enters the SOC parameter as $\lambda_{\rm SOC} \sim Z^4$ [29]. In Kondo insulators, however, a clever choice of the type of substitution has to be made. A substitution of the $4f$ element (Ce) breaks the translational symmetry of the local moment sublattice, which leads to a loss of Kondo coherence. To keep the Kondo lattice intact, substitutions should therefore be limited to the nonmagnetic elements (Bi and Pt). Most relevant for the Kondo interaction are the transition metal d electrons. Indeed, photoemission experiments evidence the presence of Pt $5d$ states near the Fermi level [30], suggesting that a substitution of Pt by another transition element would be most relevant. This is further underpinned by the fact that the Ce atoms in $Ce_3Bi_4(Pt,Pd)_3$ have only Pt (Pd) as nearest neighbors (upper right inset in Fig. 3). The second constraint is that Kondo insulators, just as heavy fermion

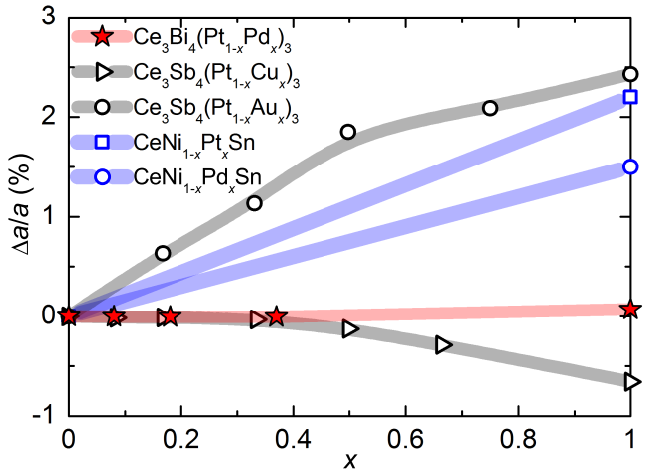

FIG. 1. (Color online) Relative change of lattice parameter a as function of the Pd content x in $Ce_3Bi_4(Pt_{1-x}Pd_x)_3$ (red), on a scale relevant to other archetypal Kondo systems [31–34] (open symbols). Lines are guides to the eyes.

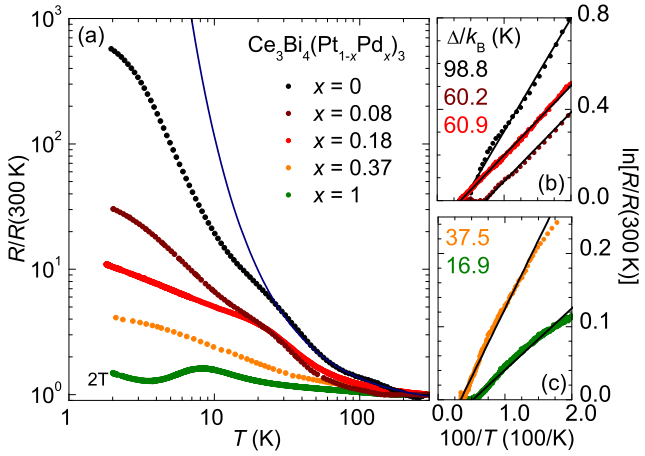

FIG. 2. (Color online) (a) Temperature-dependent electrical resistance $R(T)$, normalized to its room temperature value $R(300\,\mathrm{K})$, on a log − log scale for all investigated $Ce_3Bi_4(Pt_{1-x}Pd_x)_3$ samples. An exponentially activated resistivity, fitted to the high-temperature regime of the $x = 0$ sample, is shown as blue line. (b, c) Arrhenius plots for data above 50 K. The solid lines are the fits (see text). The data for the $x = 1$ sample were taken at 2 T to suppress a spurious superconducting resistance drop at 3 K that has no correspondence in magnetization and specific heat measurements. This magnetic field has no effect on the resistance data above 3 K.

metals, react sensitively to even small changes of chemical pressure. Thus, to keep the Kondo coupling J_K tuning minimal, isosize substitutions should be used. Finally, Kondo insulators being insulators naturally makes them react strongly to changes in electron count and thus in the chemical potential μ, which favors isoelectronic substitutions (without carrier "doping").

Previous studies have failed to separate these different effects. For instance, in the Kondo semimetal CeNiSn, isoelectronic but non-isosize substitutions of Ni by Pt or Pd close the Kondo (pseudo)gap as a consequence of the increased unit cell volume and hence the decreased J_K [31, 32]. In $Ce_3Sb_4Pt_3$, the non-isosize and non-isoelectronic substitutions of Pt by Cu and Au both suppress the Kondo insulating state although Cu doping results in a reduced [33] and Au doping in an increased unit cell volume [34]. Thus, here the change in μ dominates.

Surprisingly, no substitution series of $Ce_3Bi_4Pt_3$ other than Ce-La replacements [35, 36] have yet been studied. Here we present first results on the series $Ce_3Bi_4(Pt_{1-x}Pd_x)_3$ and show that it ideally qualifies to study pure λ_{SOC} tuning. The $4d$ transition metal Pd is much lighter than the $5d$ transition metal Pt (atomic weight 106.42 instead of 195.084) and thus an increase of the Pd content x should sizeably reduce the conduction electron λ_{SOC}. By contrast, as Pt and Pd are isoelectronic, there is minimal μ tuning. Furthermore, as will be show below, there is minimal J_K tuning.

Single crystals of $Ce_3Bi_4(Pt_{1-x}Pd_x)_3$ were grown using a modified Bi flux method [20]. The substitution levels x were determined by EDX measurements [20]. The lattice parameter a across the sample series is shown in Fig. 1. The accumulated relative change $\Delta a/a(x) = [V(x)/V(x=0)]^{1/3} - 1$, where $V(x)$ denotes the unit cell volume for a given substitution level x, is only 0.069% at $x = 1$. This is extremely small compared to substitutions in related materials (Fig. 1). Thus, unlike in these other substitution series, J_K tuning by chemical pressure can be excluded as dominating factor in $Ce_3Bi_4(Pt_{1-x}Pd_x)_3$.

Figure 2 shows the temperature dependence of the electrical resistance $R(T)$ of all investigated $Ce_3Bi_4(Pt_{1-x}Pd_x)_3$ crystals, normalized to the respective room temperature value (180 to 350 $\mu\Omega$cm, in good agreement with the published value of 220 $\mu\Omega$cm for $Ce_3Bi_4Pt_3$ [15]; small differences are attributed to the poorly defined geometrical factors of the small single crystals). With increasing x, R at low temperatures is successively reduced, corresponding to a gradual closing of the Kondo insulator gap. This can be quantified by Arrhenius fits $R = R_0 \exp[\Delta/(2k_BT)]$ to the high-temperature data [Fig. 2 (b,c)], where Δ is the gap width and k_B is the Boltzmann constant. The continuous decrease of Δ with x is shown in Fig. 3. It is remarkable that the (full) substitution of Bi by the much lighter isoelectronic element Sb has an entirely different effect: Instead of closing the Kondo insulator gap it strongly enhances it to 1080 K [34]. This must be due to the smaller size of Sb, that leads to a lattice parameter reduction by 2.3% [34], and thus a stronger hybridization, similar to the gap opening under hydrostatic pressure [18].

Gap values that are much smaller than the lower boundary of the fitting range are unphysical. This is the case for $Ce_3Bi_4Pd_3$. Its energy gap of 16.9 K should thus be taken with caution – and rather as indication for the absence of a well-defined gap (as indicated by the pink shaded region in Fig. 3). In fact, R of this sample depends only very weakly on temperature, which is characteristic of semimetals. At 8.3 K, a broad local maximum is observed. As will be shown below, this feature is echoed by features in the magnetization (Fig. 4) and spe-

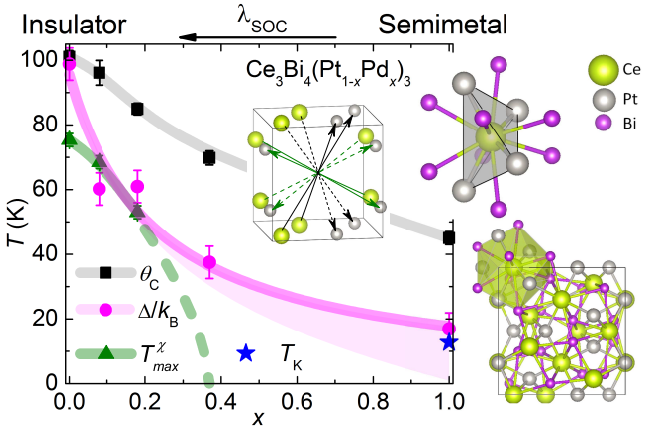

FIG. 3. (Color online) Characteristic temperature scales for $Ce_3Bi_4(Pt_{1-x}Pd_x)_3$ as function of x. $T^{\chi}_{\rm max}$ and $\Theta_{\rm C}$ are taken from Fig. 4(a) and the Curie-Weiss fits in Fig. 4(b), respectively. $\Delta/k_{\rm B}$ is taken from the Arrhenius fits in Fig. 2(b,c). The Kondo temperature $T_{\rm K}$ is taken from the entropy analysis in Fig. 5(c). The full lines are guides to the eyes. The shaded pink area represents the fact that, for $x = 1$, the Arrhenius fit loses significance and $R(T)$ becomes compatible with a gapless state (see text). The dashed green line indicates that the maximum in $\chi(T)$ is suppressed to below 2 K for $x = 0.37$. The arrow on the top axis indicates that an *in*crease of the conduction-electron $\lambda_{\rm SOC}$ (corresponding to a *de*crease of x) drives the system from a semimetallic to an insulating state. The structure sketches illustrate the unit cell (bottom), the environment of Ce with 4 nearest Pt/Pd (3.01 Å) and 8 next-nearest Bi (3.41 Å) neighbors (top), and the lack of a center of inversion for (selected) Ce and Pt atoms.

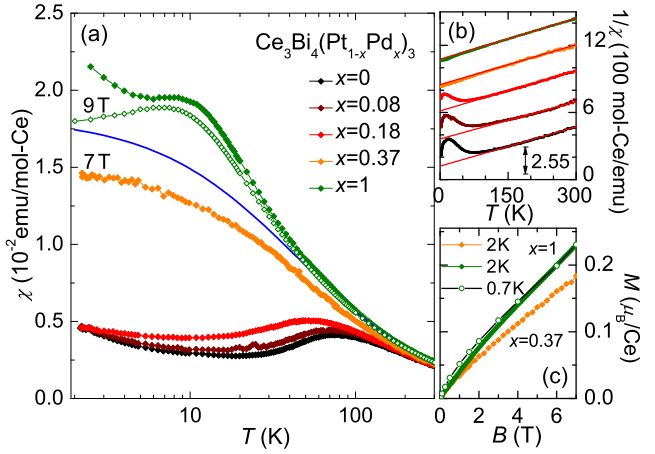

FIG. 4. (Color online) (a) Temperature-dependent magnetic susceptibility $\chi(T)$ of all investigated $Ce_3Bi_4(Pt_{1-x}Pd_x)_3$ samples, together with the Curie-Weiss fit for the $x = 1$ data (blue line, from b). (b) χ^{-1} vs T along with the Curie-Weiss fits that determine the paramagnetic Weiss temperature $\Theta_{\rm C}$. The data for $x > 0$ are successively shifted by 255 mol-Ce Oe/emu for clarity. Unless specified, the field for the data in (a) and (b) was 100 mT. (c) Selected magnetization vs field $M(B)$ isotherms. The slight nonlinearities at low fields indicate that the low-temperature upturn of $\chi(T)$, seen most clearly for the $x = 1$ sample in (a), is a readily saturable by small fields.

cific heat (Fig. 5), and is likely due to Kondo interaction in a semimetal.

The magnetic susceptibility of all investigated $Ce_3Bi_4(Pt_{1-x}Pd_x)_3$ samples [Fig. 4(a)] is well described by a Curie-Weiss law at high temperatures [Fig. 4(b)]. The effective magnetic moments, obtained by Curie-Weiss fits between 150 and 300 K, all agree within error bar with the value of 2.54 $\mu_{\rm B}$ expected for a free Ce^{3+} ion. The (negative) paramagnetic Weiss temperature $\Theta_{\rm C}$, which is a measure of the strength of antiferromagnetic (AFM) correlations driven by the Kondo interaction, decreases continuously in absolute value (Fig. 3), but remains sizeable even for the $x = 1$ sample. This is in sharp contrast to the Au-Pt and Cu-Pt substitutions in $Ce_3Sb_4Pt_3$ which suppress $-\Theta_{\rm C}$ from 647 K in $Ce_3Sb_4Pt_3$ to less than 3 K and 1 K in $Ce_3Sb_4Au_3$ [34] and $Ce_3Sb_4Cu_3$ [33], respectively.

A maximum in the magnetic susceptibility, as observed at $T^{\chi}_{\rm max} = 75$ K for the $x = 0$ sample [Fig. 4(a)], is in good agreement with previous findings [15, 17]. It signals the onset of Kondo screening associated with the opening of the Kondo insulator gap [7]. With increasing x, $T^{\chi}_{\rm max}$ is successively suppressed (Fig. 3). The $x = 0.37$ sample shows no maximum down to at least 2 K. Sample-dependent upturns of the susceptibility at the lowest temperatures, that have no correspondence in neutron scattering experiments [16], are generally attributed to a Curie tail due to a small amount of magnetic impurities.

The magnetic susceptibility of $Ce_3Bi_4Pd_3$ is qualitatively different. Below 50 K, it deviates to values larger than the Curie-Weiss law [blue line in Fig. 4(a)] and tends to saturate below 10 K, characteristics of heavy fermion metals. The upturn at the lowest temperatures is again suppressed by magnetic fields.

Further information on the nature of the ground state of $Ce_3Bi_4Pd_3$ can be extracted from specific heat $C(T)$ measurements [Fig. 5(a)]. To determine the electronic specific heat $C_{\rm el} = C - C_{\rm ph}$ of a heavy fermion material it is common practice to use the phonon specific heat $C_{\rm ph}$ as determined from its non-f reference material, which is usually well described by $C/T = \gamma + \beta T^2$. The Sommerfeld coefficient γ represents the electronic contribution and the β term the Debye approximation of the lattice contribution. Indeed, this relation holds for $La_3Bi_4Pt_3$, with $\beta = 1.46$ mJ/(mol-La K^4) [15]. The specific heat of $Ce_3Bi_4Pd_3$ displays a pronounced anomaly with respect to this Debye behavior, which is only slightly shifted to lower temperatures in a magnetic field of 7 T [Fig. 5(b)]. On the low-temperature side of the anomaly, C/T is linear in T^2, with a slope β' that is sizeably larger than that of the phonon contribution. Similar behavior was seen in the cubic heavy fermion antiferromagnet $CeIn_3$ below the Néel temperature [37, 38] and attributed to 3D AFM magnons. However, in $Ce_3Bi_4Pd_3$, there is no obvious sign of a magnetic phase transition as the observed anomalies appear too broad to represent such transitions. In addition, in view of the linear coupling of a magnetic field to a symmetry breaking order parameter, a stronger suppression would be expected if the anomaly

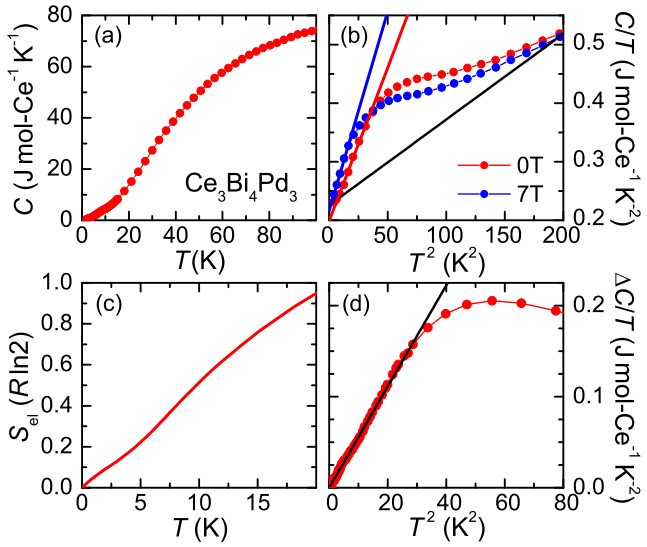

FIG. 5. (Color online) (a) Temperature-dependent specific heat $C(T)$ of $Ce_3Bi_4Pd_3$ below 100 K. (b) C/T vs T^2 below 14 K, in zero field and 7 T. The slope β of the black straight line corresponds to the phonon contribution $C_{\rm ph}$; the red and blue lines with steeper slope β' are interpreted as Weyl contributions (see text). (c) Entropy of electronic specific heat $C_{\rm el} = C - C_{\rm ph}$ vs temperature. (d) With the lowest-T CDW and NFL contributions (Supplemental Fig. S3) subtracted, linear-in-T^2 behavior (black line) of $C_{\rm el}/T$ prevails from 0.4 to 5.5 K.

indeed represented AFM ordering. Finally, the magnetic field enhances β', but would be expected to reduce it in a 3D AFM magnon scenario [39, 40].

Instead, we suggest that the $\beta' T^2$ contribution originates from bulk electronic states with linear dispersion $\varepsilon_{\mathbf{k}} = \hbar v^* k$, with the quasiparticle velocity v^*, recently predicted for a Weyl-Kondo semimetal [12]. Such states contribute a volume specific heat of $7\pi^2/30 \cdot k_B[(k_B T)/(\hbar v^*)]^3$ (Supplemental Material of [12]). From our experiments we determine $v^* = 885$ m/s which is three orders of magnitude smaller than the Fermi velocity of a simple metal. Interestingly, the (single ion) Kondo temperature $T_{\rm K}$ that we estimate as the temperature where the electronic entropy [Fig. 5(c)] reaches 0.65 ln 2 per Ce [41], is 13 K ($\sim$meV) and thus three orders of magnitude smaller than the Fermi temperature of a simple metal ($\sim$eV). This further supports the 1000-fold renormalization of the quasiparticle velocity discussed above.

The lowest-temperature $C_{\rm el}/T$ data, plotted on a logarithmic temperature scale (Supplemental Fig. S3), reveal further signs of strong correlations: A Schottky-like anomaly and a non-Fermi liquid (NFL)-like $\ln(1/T)$ upturn are discerned below 2 and 0.8 K, respectively. The former is likely a precursor of the formation of a charge density wave (CDW), a particle-hole instability that has recently been predicted for Weyl semimetals with long-range repulsive Coulomb interactions [24]. The latter may indicate that $Ce_3Bi_4Pd_3$ is close to a quantum critical point, with its Fermi level slightly away from the Weyl nodes (see [20] for further details). These observations are exciting on their own and clearly call for further studies. If we model these low-temperature contributions [orange line in Fig. S3] and subtract them from the $C_{\rm el}/T$ data, the $\beta' T^2$ term that evidences the Weyl-Kondo semimetal dispersion is seen down to the lowest temperatures [Fig. 5(d) and Supplemental Fig. S3], thus over more than a decade in temperature.

Figure 3 summarizes the effects of increasing Pd content x (bottom axis) and thus decreasing $\lambda_{\rm SOC}$ (see top axis): The absolute value of the paramagnetic Weiss temperature $\Theta_{\rm C}$ decreases with increasing x, but remains sizeable even for $x = 1$. The Kondo insulator gap Δ is reduced with increasing x and cannot be clearly discerned beyond $x = 0.37$. The spin screening temperature $T^{\chi}_{\rm max}$ is likewise reduced with x, to below 2 K for $x = 0.37$. For the semimetal $Ce_3Bi_4Pd_3$ at $x = 1$, it reappears in the form of a Kondo temperature of 13 K, as determined from the electronic entropy. This evolution, together with the above discussed thermodynamic features of $Ce_3Bi_4Pd_3$, strongly suggests that we have tuned $Ce_3Bi_4(Pt_{1-x}Pd_x)_3$ from a Kondo insulator phase for $x = 0$ to the recently predicted Weyl-Kondo semimetal phase [12] at $x = 1$. In fact, a topological Kondo insulator to Dirac-Kondo semimetal transition has recently been shown in an Anderson lattice model upon reducing $\lambda_{\rm SOC}$ [11]. For the case of a noncentrosymmetric crystal structure, a transition between a topological Kondo insulator and a Weyl-Kondo semimetal [12] may thus be theoretically expected. This exciting perspective calls for additional experiments, to further probe the topological bulk and surface states predicted for a Weyl-Kondo semimetal [12], as well as further theoretical studies on its evolution upon $\lambda_{\rm SOC}$ tuning.

Similar SOC tuning studies may also shed light on the topological nature of other strongly correlated semimetals, such as $CeRu_4Sn_6$ [42] and CeNiSn [43], that have been suggested to host topological bulk and/or surface states [27, 44, 45]. In the substitution series $Yb_3(Rh_{1-x}Ir_x)_4Ge_{13}$ a metal to AFM insulator crossover was observed with increasing x [46]. Interestingly, the Rh-Ir substitution is isoelectronic, isostructural, and almost isosize, suggestive of predominant SOC tuning, though this was not acknowledged in that work.

In conclusion we have presented noncentrosymmetric $Ce_3Bi_4(Pt_{1-x}Pd_x)_3$ as a model system for spin-orbit coupling (SOC) tuning of a Kondo insulator. A continuous decrease of the SOC strength is achieved by the isoelectronic, isostructural, and isosize substitution of the heavy 5d element Pt by the much lighter 4d element Pd on the nearest neighbor site of Ce in the crystal structure. The observed transition from a Kondo insulator to a heavy semimetal, with signatures of linearly dispersing quasiparticles of low velocity, suggests an interpretation in terms of a topological Kondo insulator to Weyl-Kondo semimetal [12] transition.We expect these findings to trigger an active search for other such tuning series, as well as experiments that further probe the newly es-

tablished Weyl-Kondo semimetal phase and the nature of its transition to the Kondo insulator phase.

We gratefully acknowledge fruitful discussions with S. E. Grefe, H.-H. Lai, and E. Morosan, helpful advice from K. Hradil, W. Artner, and D. Joshi, and financial support from the Austrian Science Fund (doctoral program W1243 and I2535-N27) and the U.S. Army Research Office (ARO Grant No. W911NF-14-1-0496) in Vienna, and the ARO (Grant No. W911NF-14-1-0525) and the Robert A. Welch Foundation (Grant No. C-1411) at Rice. The X-ray measurements were carried out at the X-Ray Center, Vienna University of Technology.

*Corresponding author: paschen@ifp.tuwien.ac.at

[1] See, e.g., Focus Issue "Topological matter", Nat. Phys. **12**, No. 7, pp. 615-718 (2016).
[2] M. Z. Hasan and C. L. Kane, Rev. Mod. Phys. **82**, 3045 (2010).
[3] X.-L. Qi and S.-C. Zhang, Rev. Mod. Phys. **83**, 1057 (2011).
[4] See, e.g., Focus Issue "Topological semimetals", Nat. Mater. **15**, No. 11 (2016).
[5] R. Schaffer, E. K.-H. Lee, B.-J. Yang, and Y. B. Kim, Rep. Prog. Phys. **79**, 094504 (2016).
[6] G. Aeppli and Z. Fisk, Comments Condens. Matter Phys. **16**, 155 (1992).
[7] P. S. Riseborough, Adv. Phys. **49**, 257 (2000).
[8] M. Dzero, K. Sun, V. Galitski, and P. Coleman, Phys. Rev. Lett. **104**, 106408 (2010).
[9] M. Dzero, J. Xia, V. Galitski, and P. Coleman, Annu. Rev. Condens. Matter Phys. **7**, 249 (2016).
[10] X.-Y. Feng, J. Dai, C.-H. Chung, and Q. Si, Phys. Rev. Lett. **111**, 016402 (2013).
[11] X.-Y. Feng, H. Zhong, J. Dai, and Q. Si, Dirac-Kondo semimetals and topological Kondo insulators in the dilute carrier limit, arXiv:1605.02380, 2016.
[12] H.-H. Lai, S. E. Grefe, S. Paschen, and Q. Si, Weyl-Kondo semimetal in a heavy fermion system, arXiv:1612.03899v1, 2016.
[13] H. v. Löhneysen, A. Rosch, M. Vojta, and P. Wölfle, Rev. Mod. Phys. **79**, 1015 (2007).
[14] Q. Si and S. Paschen, Phys. Status Solidi B **250**, 425 (2013).
[15] M. F. Hundley, P. C. Canfield, J. D. Thompson, Z. Fisk, and J. M. Lawrence, Phys. Rev. B **42**, 6842 (1990).
[16] A. Severing, J. D. Thompson, P. C. Canfield, Z. Fisk, and P. Riseborough, Phys. Rev. B **44**, 6832 (1991).
[17] B. Bucher, Z. Schlesinger, P. C. Canfield, and Z. Fisk, Phys. Rev. Lett. **72**, 522 (1994).
[18] J. C. Cooley, M. C. Aronson, and P. C. Canfield, Phys. Rev. B **55**, 7533 (1997).
[19] M. Jaime, R. Movshovich, G. Stewart, W. Beyermann, M. Berisso, M. Hundley, P. Canfield, and J. Sarrao, Nature **405**, 160 (2000).
[20] See Supplemental Material [url] for further information on methods, crystal growth, structural and chemical analyses, and thermodynamic properties below 2 K, which includes Refs. [21-26].
[21] P. C. Canfield and Z. Fisk, Philos. Mag. B **65**, 1117 (1992).
[22] F. Han, X. Wan, D. Phelan, C. C. Stoumpos, M. Sturza, C. D. Malliakas, Q. Li, T.-H. Han, Q. Zhao, D. Y. Chung, and M. G. Kanatzidis, Phys. Rev. B **92**, 045112 (2015).
[23] W. Hermes, S. Linsinger, R. Mishra, and R. Pöttgen, Monatsh. Chem. **139**, 1143 (2008).
[24] H. Wei, S.-P. Chao, and V. Aji, Phys. Rev. B **89**, 235109 (2014).
[25] Y. Luo, F. Ronning, N. Wakeham, X. Lu, T. Park, Z.-A. Xu, and J. D. Thompson, Proc. Natl. Acad. Sci. USA **112**, 13520 (2015).
[26] J. Custers, K. Lorenzer, M. Müller, A. Prokofiev, A. Sidorenko, H. Winkler, A. M. Strydom, Y. Shimura, T. Sakakibara, R. Yu, Q. Si, and S. Paschen, Nature Mater. **11**, 189 (2012).
[27] P.-Y. Chang, O. Erten, and P. Coleman, Möbius Kondo insulators, arXiv: 1603.03435v2, 2016.
[28] N. Wakeham, P. F. S. Rosa, Y. Q. Wang, M. Kang, Z. Fisk, F. Ronning, and J. D. Thompson, Phys. Rev. B **94**, 035127 (2016).
[29] K. V. Shanavas, Z. S. Popović, and S. Satpathy, Phys. Rev. B **90**, 165108 (2014).
[30] Y. Takeda, M. Arita, Y. Okamura, H. Sato, K. Shimada, K. Mamiya, H. Namatame, M. Taniguchi, K. Katoh, F. Iga, and T. Takabatake, Jpn. J. Appl. Phys. **38**, 209 (1999).
[31] S. Nishigori, H. Goshima, T. Suzuki, T. Fujita, G. Nakamoto, T. Takabatake, H. Fujii, and J. Sakurai, Physica B **186 & 188**, 406 (1993).
[32] M. Kasaya, T. Tani, F. Iga, and T. Kasuya, J. Magn. Magn. Mater. **76**, 278 (1988).
[33] C. D. W. Jones, K. A. Regan, and F. J. DiSalvo, Phys. Rev. B **60**, 5282 (1999).
[34] K. Katoh and M. Kasaya, J. Phys. Soc. Jpn. **65**, 3654 (1996).
[35] P. Schlottmann, Phys. Rev. B **46**, 998 (1992).
[36] T. Pietrus, H. Löhneysen, and P. Schlottmann, Phys. Rev. B **77**, 115134 (2008).
[37] A. Berton, J. Chaussy, G. Chouteau, B. Cornut, J. Flouquet, J. Odin, J. Palleau, J. Peyrard, and R. Tournier, J. Phys. Colloq. **40**, C5 (1979).
[38] A. L. Cornelius, P. G. Pagliuso, M. F. Hundley, and J. L. Sarrao, Phys. Rev. B **64**, 144411 (2001).
[39] S. Deonarine and S. J. Joshua, Phys. Stat. Solidi (b) **57**, 767 (1973).
[40] M. B. Maple, N. P. Butch, N. A. Frederick, P.-C. Ho, J. R. Jeffries, T. A. Saylesa, T. Yanagisawa, W. M. Yuhasz, S. Chi, H. J. Kang, J. W. Lynn, P. Dai, S. K. McCall, M. W. McElfresh, M. J. Fluss, Z. Henkie, and A. Pietraszko, Proc. Natl. Acad. Sci. USA **103**, 6783 (2006).
[41] H.-U. Desgranges and K. Schotte, Phys. Lett. A **91**, 240 (1982).
[42] V. Guritanu, P. Wissgott, T. Weig, H. Winkler, J. Sichelschmidt, M. Scheffler, A. Prokofiev, S. Kimura, T. Iizuka, A. M. Strydom, M. Dressel, F. Steglich, K. Held, and S. Paschen, Phys. Rev. B **87**, 115129 (2013).
[43] U. Stockert, P. Sun, N. Oeschler, F. Steglich, T. Takabatake, P. Coleman, and S. Paschen, Phys. Rev. Lett. **117**, 216401 (2016).

[44] M. Sundermann, F. Strigari, T. Willers, H. Winkler, A. Prokofiev, J. M. Ablett, J. P. Rueff, D. Schmitz, E. Weschke, M. Moretti Sala, A. Al-Zein, A. Tanaka, M. W. Haverkort, D. Kasinathan, L. H. Tjeng, S. Paschen, and A. Severing, Sci. Rep. **5**, 17937 (2015).

[45] Y. Xu, C. Yue, H. Weng, and X. Dai, Heavy Weyl fermion state in $CeRu_4Sn_6$, arXiv: 1608.04602, 2016.

[46] B. K. Rai, I. W. H. Oswald, J. Y. Chan, and E. Morosan, Phys. Rev. B **93**, 035101 (2016).